The Astronomical Journal, 131:1674–1686, 2006 March

A CATALOG OF SPECTROSCOPICALLY SELECTED CLOSE BINARY SYSTEMS FROM THE SLOAN DIGITAL SKY SURVEY DATA RELEASE FOUR

Nicole M. Silvestri,[1] Suzanne L. Hawley,[1] Andrew A. West,[1] Paula Szkody,[1] John J. Bochanski,[1] Daniel J. Eisenstein,[2] Peregrine McGehee,[3,4] Gary D. Schmidt,[2] J. Allyn Smith,[5] Michael A. Wolfe,[1] Hugh C. Harris,[6] Scot J. Kleinman,[7] James Liebert,[2] Atsuko Nitta,[7] J. C. Barentine,[7] Howard J. Brewington,[7] John Brinkmann,[7] Michael Harvanek,[7] Jurek Krzesiński,[7,8] Dan Long,[7] Eric H. Neilsen, Jr.,[7,9] Donald P. Schneider,[10] and Stephanie A. Snedden[7]

Received 2005 October 5; accepted 2005 October 27

ABSTRACT

We present a spectroscopic sample of 747 detached close binary systems from the Sloan Digital Sky Survey (SDSS) Fourth Data Release. The majority of these binaries consist of a white dwarf primary and a low-mass secondary (typically M dwarf) companion. We have determined the temperature and gravity for 496 of the white dwarf primaries and the spectral type and magnetic activity properties for 661 of the low-mass secondaries. We have estimated the distances for each of the white dwarf–main-sequence star binaries and use white dwarf evolutionary grids to establish the age of each binary system from the white dwarf cooling times. With respect to a spectroscopically identified sample of ~8000 isolated M dwarf stars in the SDSS, the M dwarf secondaries show enhanced activity with a higher active fraction at a given spectral type. The white dwarf temperatures and gravities are similar to the distribution of ~1900 DA white dwarfs from the SDSS. The ages of the binaries in this study range from ~0.5 Myr to nearly 3 Gyr (average age ~0.20 Gyr).

Key words: binaries: close — novae, cataclysmic variables — stars: activity — stars: low-mass, brown dwarfs — white dwarfs

Online material: color figure, machine-readable tables

1. INTRODUCTION

One of the many interesting by-products of the Sloan Digital Sky Survey (SDSS; York et al. 2000) is the detection of a large number of unresolved, close binary star systems. In particular, the five-color photometry and spectra covering nearly the entire optical wavelength range permit easy identification of unresolved binaries consisting of a (blue) white dwarf primary and a (red) secondary star, typically a low-mass main-sequence M dwarf. These binary systems represent the likely progenitor population to most cataclysmic variables (CVs) and perhaps Type Ia supernovae and are therefore a subject of keen interest. In addition, they provide an interesting test of stellar evolution for both the primary and secondary stars in the binary environment. Recent SDSS surveys of white dwarfs (Kleinman et al. 2004, hereafter K04; Eisenstein et al. 2005) and M dwarfs (West et al. 2004, hereafter W04) have summarized the bulk properties of these nearby stellar populations as they evolve in isolation. Here we present a large sample of white dwarf–M dwarf (WDM) binaries identified spectroscopically in the SDSS through the Fourth Data Release (Adelman-McCarthy et al. 2006, hereafter DR4). We discuss the sample selection, provide tables of the properties of the individual components of each system (e.g., temperature, gravity, and age for the white dwarfs; spectral type, Hα emission, equivalent width, and spectroscopic parameters for the M dwarfs), and compare the properties to those of the isolated white dwarf (K04) and M dwarf surveys (W04). In subsequent papers we will (1) explore the presence of magnetic white dwarfs in these systems and the implications for the production of magnetic CVs and (2) consider a subset of the sample for which we have extensive radial velocity information (and hence periods) to understand in detail the changes that occur as the stars lose angular momentum and decrease their orbital separation, evolving into yet closer binary systems, some on their way to the CV phase of evolution.

Most previous attempts to identify and study white dwarf binaries with low-mass companions have been confined to wide, common proper motion systems (see Luyten 1963; Oswalt et al. 1996; Silvestri et al. 2001, 2002) where the evolution of the system proceeds as for single stars due to the large (~10^3 AU) orbital separation of the components. Studies of pre-CVs such as Schultz et al. (1996), Vennes et al. (1999), Marsh (2000), Hillwig et al.

[1] Department of Astronomy, University of Washington, Box 351580, Seattle, WA 98195; nms@astro.washington.edu, slh@astro.washington.edu, west@astro.washington.edu, szkody@astro.washington.edu, bochansk@astro.washington.edu, maw2323@u.washington.edu.

[2] Department of Astronomy and Steward Observatory, University of Arizona, Tucson, AZ 85721; eisenste@cmb.as.arizona.edu, jliebert@as.arizona.edu, schmidt@as.arizona.edu.

[3] Los Alamos National Laboratory, LANSCE-8, MS H82, Los Alamos, NM 87545; peregrin@apo.nmsu.edu.

[4] Department of Astronomy, New Mexico State University, P.O. Box 30001, Department 4500, Las Cruces, NM 88003; peregrin@apo.nmsu.edu.

[5] Los Alamos National Laboratory, ISR-4, MS D448, Los Alamos, NM 87545; jasman@nis.lanl.gov.

[6] US Naval Observatory, P.O. Box 1149, Flagstaff, AZ 86002; hch@nofs.navy.mil.

[7] New Mexico State University, Apache Point Observatory, P.O. Box 59, Sunspot, NM 88349; sjnk@apo.nmsu.edu, ank@apo.nmsu.edu, jcb@apo.nmsu.edu, hbrewington@apo.nmsu.edu, jb@apo.nmsu.edu, harvanek@apo.nmsu.edu, jurek@apo.nmsu.edu, long@apo.nmsu.edu, neilsen@fnal.gov, snedden@apo.nmsu.edu.

[8] Mount Suhoro Observatory, Cracow Pedagogical University, Ul. Podchorazych 2, 30-084 Cracow, Poland; jurek@apo.nmsu.edu.

[9] Fermi National Accelerator Laboratory, P.O. Box 500, Batavia, IL 60510; neilsen@fnal.gov.

[10] Department of Astronomy and Astrophysics, Pennsylvania State University, University Park, PA 16802; dps@miffy2.astro.psu.edu.

Report Documentation Page

Form Approved
OMB No. 0704-0188

1. REPORT DATE	2. REPORT TYPE	3. DATES COVERED
2006	**N/A**	**-**

4. TITLE AND SUBTITLE	5a. CONTRACT NUMBER
A Catalog of Spectroscopically Selected Close Binary Systems From the Sloan Digital Sky Survey Data Release Four	5b. GRANT NUMBER
	5c. PROGRAM ELEMENT NUMBER
6. AUTHOR(S)	5d. PROJECT NUMBER
	5e. TASK NUMBER
	5f. WORK UNIT NUMBER
7. PERFORMING ORGANIZATION NAME(S) AND ADDRESS(ES) **Library U.S. Naval Observatory 3450 Massachusetts Avenue, N.W. Washington, DC 20392-5420**	8. PERFORMING ORGANIZATION REPORT NUMBER
9. SPONSORING/MONITORING AGENCY NAME(S) AND ADDRESS(ES)	10. SPONSOR/MONITOR'S ACRONYM(S)
	11. SPONSOR/MONITOR'S REPORT NUMBER(S)

12. DISTRIBUTION/AVAILABILITY STATEMENT
Approved for public release, distribution unlimited

13. SUPPLEMENTARY NOTES

14. ABSTRACT

15. SUBJECT TERMS

16. SECURITY CLASSIFICATION OF:			17. LIMITATION OF ABSTRACT	18. NUMBER OF PAGES	19a. NAME OF RESPONSIBLE PERSON
a. REPORT	b. ABSTRACT	c. THIS PAGE			
unclassified	**unclassified**	**unclassified**	**SAR**	**13**	

(2000), Maxted et al. (2004), and most recently Morales-Rueda et al. (2005) and Dobbie et al. (2005) involve too few systems for robust statistical study. Raymond et al. (2003) carried out a preliminary survey of WDM systems in the SDSS using data from the Early Data Release (Stoughton et al. 2002, hereafter EDR) and Data Release One (Abazajian et al. 2003). Their sample comprised 109 systems, of which 106 are contained in our sample (the remaining three have been reclassified and do not fit our sample criteria). Our much larger sample and improved analysis enables us to extend and refine their results. We anticipate that approximately 500 additional systems will be added to the sample by the end of the SDSS. The new Sloan Extension for Galactic Understanding and Exploration (SEGUE) is continuing to target these objects and will likely discover more of these close binaries at lower Galactic latitudes.

The paper proceeds as follows. In § 2 we describe the sample selection and present extensive tables giving the full photometric and spectroscopic description of the systems. In § 3 we derive basic parameters for the white dwarf primaries and compare these with the extensive survey of white dwarfs in the SDSS (K04). Section 4 contains a discussion of the M dwarf secondaries and comparison to the SDSS survey of M dwarfs in W04. Section 5 summarizes our conclusions and plans for future work.

2. WDM SAMPLE SELECTION

This study represents a compilation of ~750 close binary systems observed by the SDSS through the DR4. The SDSS (York et al. 2000; EDR; Abazajian et al. 2003, 2004, 2005; Adelman-McCarthy et al. 2006) is an imaging and spectroscopic survey of 10^4 deg^2 of sky in five colors (u, g, r, i, and z; Fukugita et al. 1996; Gunn et al. 1998, 2005). Details on the image processing and calibration for the SDSS can be found in Fan (1999), Lupton et al. (1999), Hogg et al. (2001), Smith et al. (2002), Pier et al. (2003), Ivezić et al. (2004), and Tucker et al. (2005). Objects selected for follow-up spectroscopy are obtained with twin fiber-fed double spectrographs, which cover a wavelength range of 3800 to ~10,000 Å.

We restrict the sample to systems that have been observed spectroscopically, are detached (no observational signature of mass transfer or an accretion disk), contain a white dwarf primary,[11] and are in an unresolved binary[12] with a low-mass, nondegenerate companion. An example spectrum of a WDM system is shown in Figure 1. The top panel displays an SDSS spectrum of an unresolved, close binary system consisting of a blue, white dwarf primary and a red, M dwarf secondary. The observed spectrum is the superposition of the unresolved spectral energy distributions of the two components. The bottom panels (described in more detail in § 2.1) show the spectra of the recovered white dwarf (*left*) and the recovered M dwarf (*right*). Note the chromospheric emission from the magnetically active M dwarf seen in the Hα (~6563 Å) line in the bottom right panel. The M dwarf Hα emission may also be seen superposed on the Hα absorption line of the white dwarf in the top panel.

As described in Raymond et al. (2003), an initial set of photometric selection criteria was developed to identify these systems using SDSS photometry. Four colors ($u - g < 0.45$ [blue], $g - r < 0.70$ [blue], $r - i > 0.30$ [red], and $i - z > 0.40$ [red]) yield reliable identification to a limiting magnitude of $g < 20$. The color cuts were later refined [$(u - g) - 1.314(g - r) < 0.61$, $(r - i) > 0.91$, $(i - z) > 0.49$] to improve the selection of these pairs (P. McGehee 2005, private communication). While this targeting algorithm is relatively efficient, it is of low priority in the overall SDSS spectroscopic targeting pipeline, and the resulting spectra obtained during normal survey operations represent only a small fraction (<20%) of our SDSS spectroscopic sample. The colors of white dwarf–dominated unresolved pairs are similar to many other interesting cosmological objects targeted by the SDSS; hence, the majority of systems in this sample were serendipitously targeted for spectroscopy by other higher priority pipelines (e.g., quasars, white dwarfs). Therefore, our spectroscopic compilation of close binary systems is not well defined photometrically, nor is it statistically complete.

The similarity in color to so many different objects targeted by the SDSS makes the task of identifying these objects based solely on their *ugriz* photometry quite difficult. Typical color cuts (see Smolčić et al. 2004) do not single out the pairs in which the flux is very blue (dominated by the flux from the white dwarf) or very red (dominated by the flux from the M dwarf). The final color cuts for the spectroscopic targeting algorithm were necessarily quite narrow in order to avoid severe contamination by isolated white dwarfs and by M dwarfs from the low-mass end of the stellar locus. Searching the SDSS spectroscopic database only for objects with this stringent color selection would exclude many systems.

Instead, we resorted to an initial visual inspection of each of the 640 fibers from each of the ~1000 DR4 plates in an effort to recover more spectroscopically observed pairs. The obviously time-consuming nature of this process prompted the creation of an algorithm that we used to automatically search each spectrum for a variety of hydrogen (Balmer Hα, Hβ, Hγ) and helium absorption features that identify white dwarfs. We also searched for emission features to find active M dwarfs and CVs. Each selected spectrum is checked by eye, and if it is a bona fide WDM pair, each binary component is assigned a coarse identification. The WDM pairs with low signal-to-noise ratio (S/N < 5) or non-DA/DB primaries are missed by our algorithm, but many have been recovered through the white dwarf identification pipeline described in K04 and Eisenstein et al. (2005). Therefore, we believe our sample comprises almost all of the spectroscopically observed WDM binaries in the SDSS through the DR4 data release (2005 July).

Table 1 lists the SDSS photometry (*psfmag*) for the entire sample, including 106 of the 109 pairs from Raymond et al. (2003). Columns (1)–(4) give the SDSS coordinate name (hhmmss.ss± ddmmss.s J2000.0), plate number, fiber number, and Modified Julian Date (MJD) of the observation, respectively. Column (5) lists the coarse identifications of each component of the pair; columns (6) and (7) list the right ascension (J2000.0 in decimal hr) and declination of the object (J2000.0 in decimal degrees); columns (8)–(22) give the *ugriz* magnitudes, errors, and Galactic extinctions; column (23) lists the original data release; and column (24) lists additional notes. We follow the convention of designating uncertain spectral type classification with a colon; i.e., any spectral type followed immediately by a colon indicates uncertainty in the by-eye classification of the object. For example, DA:+dM indicates that the most likely spectral type for the white dwarf primary is DA, although for various reasons (most commonly low S/N) the classification should be taken as tentative until follow-up spectroscopy can be performed. We maintain this notation in all tables. It should be noted that the classifications in this paper supersede the more general classifications presented in Eisenstein et al. (2005). Updated classifications for these objects are presented in §§ 3 and 4 (Tables 4 and 5).

[11] We define the white dwarf, the original high-mass component, as the primary in these systems, unlike wide binary systems where the primary is typically defined as the brighter of the two components.

[12] A parallel investigation of common proper motion binary systems in the SDSS is underway, and we refer the reader to Smith et al. (2004) for details.

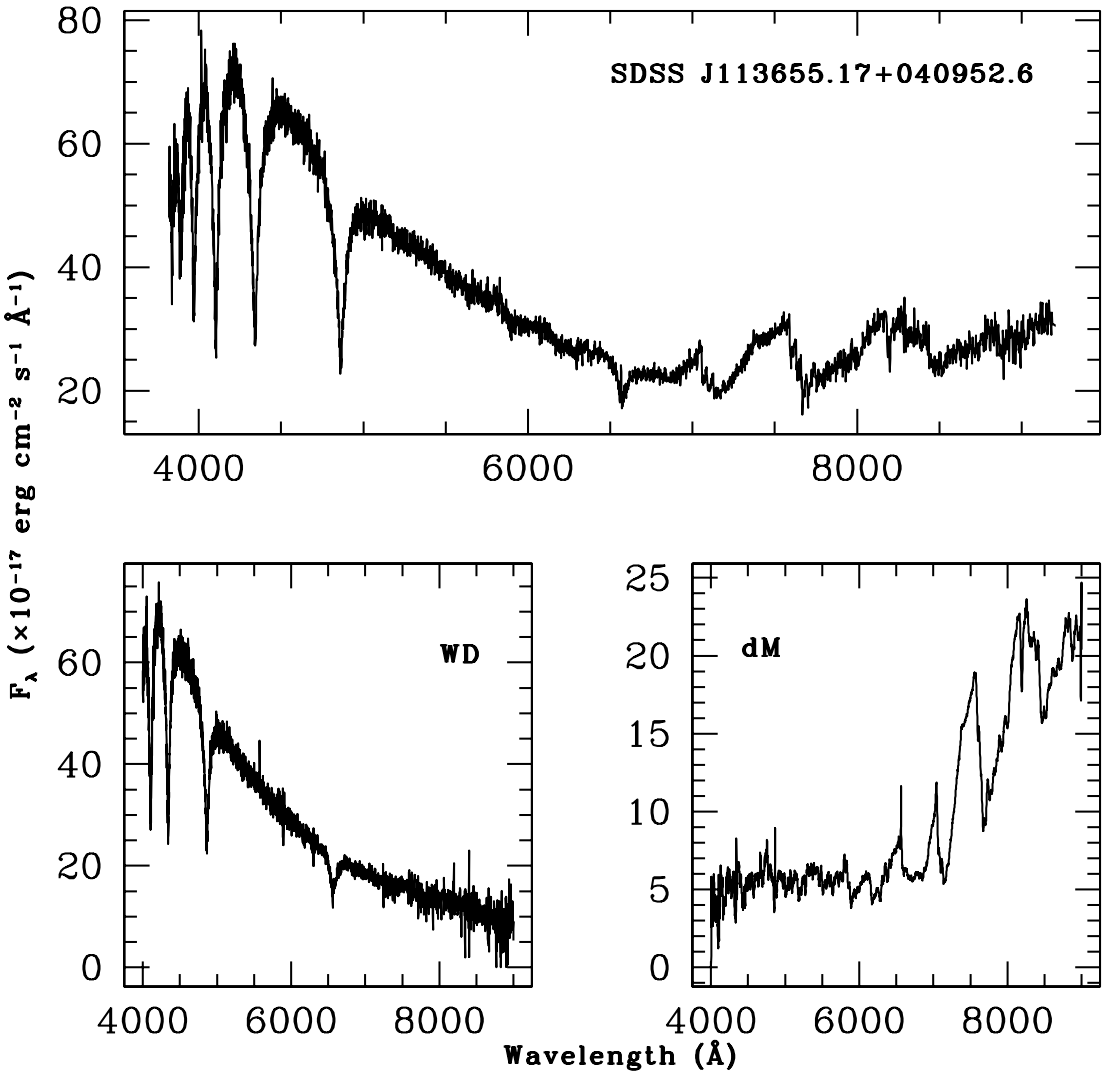

FIG. 1.—*Top*: Spectrum of the unresolved close binary system SDSS J113655.17+040952.6; $R \sim 1800$. *Bottom left*: Spectrum of the recovered white dwarf. *Bottom right*: Recovered M dwarf.

Updated photometry and spectroscopy from SDSS data releases beyond the EDR led to the reclassification of three of the 109 objects from the Raymond et al. (2003) sample. New photometry and tentative spectral types are given in Table 1 for SDSS J143947.62−010606.9 (DA+:e) and SDSS J234459.62+002749.9 (DA+:). The object SDSS J113722.25+014848.6 is the CV RZ Leo; details can be found in Szkody et al. (2003). As this system is undergoing mass transfer, we exclude it from our sample.

Figures 2 and 3 show the *ugr* and *gri* color-color diagrams for the spectroscopically identified WDMs (*open circles in both figures*), as compared to the photometrically identified WDMs of Smolčić et al. (2004; *dots in both figures*) and the spectroscopically identified white dwarfs of K04 (*crosses in both figures*). The colors are the point-spread function (PSF) magnitudes from the latest version of the photometry pipeline (photo 5.4.25; Lupton et al. 2001), as described by Fukugita et al. (1996), Gunn et al. (1998), Hogg et al. (2001), Smith et al. (2002), and EDR. They have been corrected for Galactic extinction (Schlegel et al. 1998); this correction is usually minor for these relatively nearby systems. The contribution from the M dwarf companion skews the location of the pairs in color-color space to redder colors in both figures from the locus occupied by isolated DA white dwarfs. Very few of the red (M dwarf–dominated) WDMs that are seen photometrically by Smolčić et al. (2004) are recovered spectroscopically, most likely because they are not targeted with the same frequency as the bluer WDMs that more closely match the colors of high-priority targets in the main SDSS. Smolčić et al. (2004) used strict color cuts to avoid contamination of their sample by white dwarfs and quasars. The cuts are most obvious in Figure 3 and account for the abrupt termination of the sample (*dots*) above the DA white dwarfs in the figure. The spectroscopically identified sample of WDMs fills the gap between the photometrically identified samples of white dwarfs and WDMs, recovering many objects that would have been missed by the photometric cuts for either survey.

2.1. *Separating the Components of the WDM Systems*

To investigate the properties of the individual components of the WDM binary systems, we need a robust method of separating the two stellar spectra for individual analysis. Our method uses M star templates and color indices as described in Hawley et al. (2002) and the white dwarf model atmospheres of D. Koester, described in K04 and Eisenstein et al. (2005). We use an iterative χ^2 method to fit and subtract white dwarf models and M dwarf templates from each WDM spectrum to find the best fit model and template for the white dwarf and M dwarf, respectively.

TABLE 1

SDSS White Dwarf + Main-Sequence Star Binaries

Name (SDSS J) (1)	Plate (2)	Fiber (3)	MJD (4)	Spectral Type[a] (SP1 + SP2) (5)	R.A.[b] (deg) (6)	Decl. (deg) (7)	u_{psf} (8)	σ_u (9)	A_u (10)	g_{psf} (11)	σ_g (12)	A_g (13)	r_{psf} (14)	σ_r (15)	A_r (16)	i_{psf} (17)	σ_i (18)	A_i (19)	z_{psf} (20)	σ_z (21)	A_z (22)	Data Release[c] (23)	Notes[d] (24)
001029.87+003126.2	0388	545	51793	DZ: + dM	2.62448	00.52396	21.93	0.19	0.14	20.85	0.04	0.10	19.98	0.03	0.08	19.00	0.02	0.06	18.42	0.04	0.04	EDR	
001324.33−085021.4	0652	321	52138	WD: + dM	3.35139	−08.83929	19.69	0.05	0.16	19.73	0.03	0.12	19.67	0.03	0.09	19.08	0.03	0.07	18.57	0.04	0.05	DR1	
001726.63−002451.2	0687	153	52518	DA + dMe	4.36099	−00.41422	19.68	0.04	0.14	19.29	0.03	0.10	19.03	0.02	0.07	18.19	0.02	0.06	17.54	0.03	0.04	R	
001733.59+004030.4	0389	614	51795	DA + dM	4.38996	00.67511	22.10	0.40	0.13	20.79	0.14	0.10	19.59	0.03	0.07	18.17	0.02	0.05	17.39	0.02	0.04	EDR/R	
001749.24−000955.3	0389	112	51795	DA + dMe	4.45519	−00.16539	16.57	0.02	0.13	16.87	0.02	0.10	17.03	0.01	0.07	16.78	0.01	0.05	16.47	0.02	0.04	EDR/R	

Notes.—Table 1 is published in its entirety in the electronic edition of the *Astronomical Journal*. A portion is shown here for guidance regarding its form and content.

[a] Spectral type; initial identification; e: emission detected by eye.

[b] Right ascension and declination are J2000.0 equinox.

[c] (R) Originally published in Raymond et al. (2003); (K) originally published in K04. Numbers in parentheses are plate numbers for the object's original data release.

[d] Double asterisks indicate potential low-gravity ($\log g < 7$) white dwarfs.

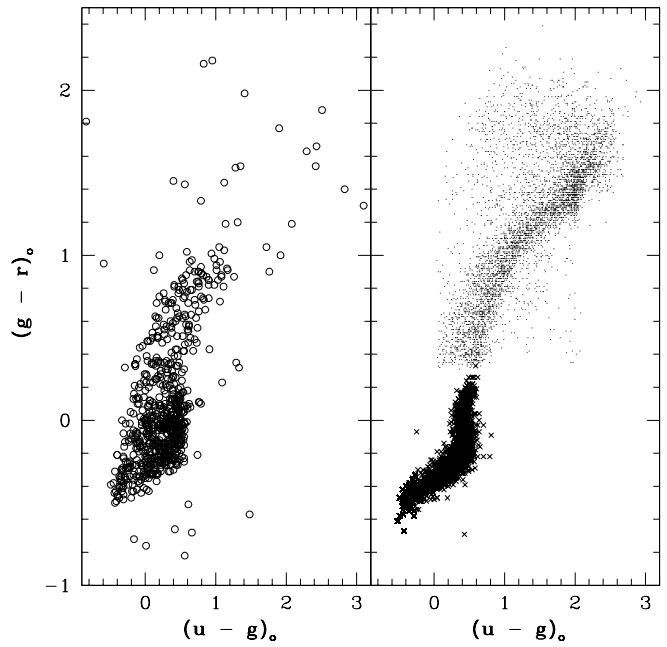

FIG. 2.—The *ugr* color-color diagram for the WDMs in our sample. The spectroscopically identified WDMs are plotted as open circles (*left*). For comparison, in the right panel we plot the photometrically identified WDMs of Smolčić et al. (2004; *dots*) and the isolated white dwarfs of K04 (*crosses*).

An example of this subtraction process is introduced in Figure 1. The WDM, SDSS J113655.17+040952.6 (*top*), was separated into its two component stars by subtracting a best-fit model DA white dwarf with $T_{\rm eff} \sim 13{,}000$ K and $\log g = 8.0$ from the original spectrum to reveal the M dwarf. A best-fit M5 template was then subtracted from the original spectrum to reveal the white dwarf. The process works quite well with minimal smoothing (maximum boxcar of 7 Å for spectra with S/N > 10). The separated white dwarf and M dwarf spectra are then processed and analyzed independently, as described in § 3 (for the white dwarfs) and § 4 (for the M dwarfs).

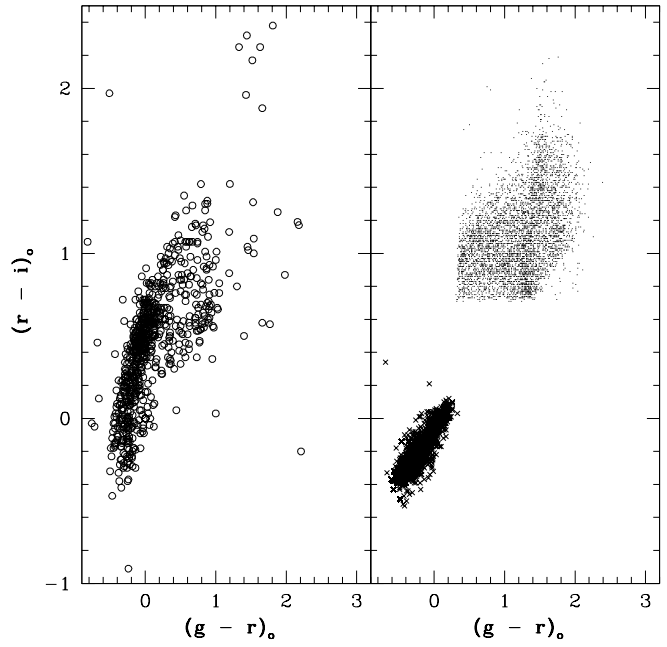

FIG. 3.—The *gri* color-color diagram for the WDMs in our sample. The spectroscopically identified WDMs are plotted as open circles (*left*). For comparison, in the right panel we plot the photometrically identified WDMs of Smolčić et al. (2004; *dots*) and the isolated white dwarfs of K04 (*crosses*).

TABLE 2
SDSS WHITE DWARF SPECTRAL TYPES

Spectral Type	Number of Components
DA(B, H)	666(6, 3)
DB(A)	26(2)
DC	16
DZ(A)	5(1)
DO	1
DQ	1
WD[a]	31

NOTES.—Atmospheric composition classification. Refer to § 3.1 and Table 5 for spectral subtypes. Letters and numbers in parentheses indicate multiple atmospheric components. For example, DB(A) and 26(2) indicate that 26 white dwarfs are classified as DB and two are of mixed atmosphere type DBA.

[a] WD: unclassified. Detected the presence of a hot, blue companion but could not classify the spectral type. Refer to § 3 for details.

3. THE WHITE DWARF PRIMARIES

The overwhelming majority of the white dwarf primaries are hydrogen-atmosphere, DA white dwarfs. The handful of non-DA primaries are of types DB, DC, DZ, DO, and DBA. Table 2 lists the number of white dwarfs of each spectral type in the current sample (see Table 3 for the breakdown of M dwarf spectral types).

Following the prescription outlined in K04 and implementing their `autofit` program, the spectra are fitted to the temperature–surface gravity grid of theoretical pure hydrogen and pure helium white dwarf model spectra of D. Koester (see Finley et al. [1997] and K04 for a full description of the models and `autofit` program), with 6000 K < $T_{\rm eff}$ < 100,000 K and $\log g$ from 5 to 9. Our white dwarf spectral type identifications follow the convention of Sion et al. (1983). An example of one of our

TABLE 3
SDSS M DWARF SPECTRAL TYPES

Spectral Type	Number of Components
K0	1
K5	4
K7	27
M0	64
M1	42
M2	81
M3	149
M4	179
M5	66
M6	33
M7	8
M8	2
M9/L0	5
M:[a]	67
C	3
:[b]	15

NOTES.—Final classification. Refer to § 4 for details.

[a] M: Unclassified. Detected the presence of a red companion but could not classify the spectral type. Refer to § 4 for details.

[b] Red excess detected in photometry and /or emission detected in WD spectra. Suspect presence of a companion but need spectroscopic follow-up to confirm.

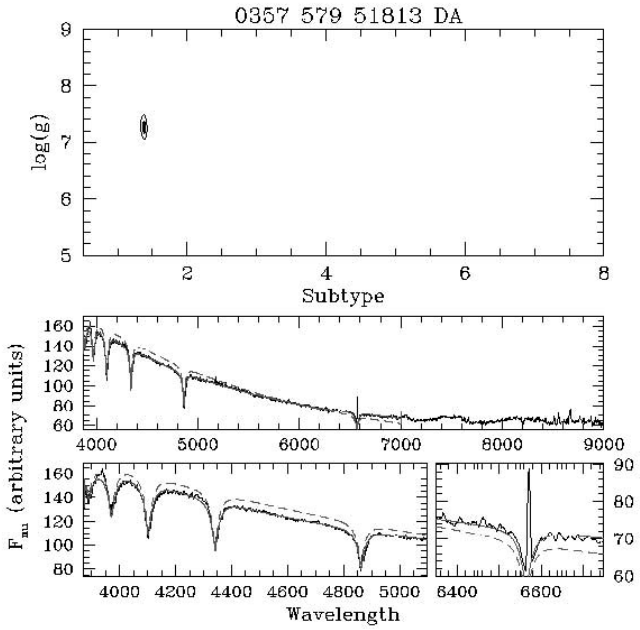

FIG. 4.—WDM SDSS J172406.14+562003.1 from our sample. D. Koester's DA white dwarf atmospheric model fit to the spectrum is shown with reddening (*solid line*) and without refluxing/reddening (*dashed line*). The white dwarf has $T_{\rm eff} = 36{,}250$ K and $\log g = 7.2$, with a final spectral type of DA1.4. Note the excellent fit even with the strong Hα emission and residual features in the red from the companion M dwarf, which were not perfectly subtracted from the spectrum. [*See the electronic edition of the Journal for a color version of this figure.*]

fits from the `autofit` program is given in Figure 4. The top panel displays the likelihood contours (1, 2, 3, 5, and 10 σ) in $\log g$-subtype space, where the subtype represents the $T_{\rm eff}$ of the white dwarf in units of $50{,}400/T_{\rm eff}$ (Sion et al. 1983). The middle and bottom panels plot the full SDSS spectrum and the regions of the white dwarf spectrum where interesting features are typically located (e.g., Balmer hydrogen and helium absorption). The solid line is the fit that includes reddening, and the dashed line is the fit without reddening/refluxing (see K04 for details).

The SDSS PSF magnitudes of the WDM pairs are used in the overall fit, as for the single white dwarfs described in K04. We make no effort to deconvolve the white dwarf's color contribution from the M dwarf's color contribution. The fits are quite good if the continuum contribution from the M dwarf and contamination of the Hα absorption feature are small (or effectively removed) and the spectrum is of high quality (S/N $\geq$ 15). In some cases, residual M dwarf flux (as seen in Fig. 4 between $\sim$7000 and 9000 Å) remains in the spectrum. Our fits to the spectra were applied between 3500 and 5400 Å. This excludes both the $\sim$7000–9000 Å region discussed above and Hα, which tends to be most contaminated by the M dwarf and is the feature least likely to be recovered in the subtraction process. Tests on isolated white dwarfs from the K04 study that exclude Hα from the fit show very little change in the measured $T_{\rm eff}$ and $\log g$ determined by the `autofit` program. The change in $T_{\rm eff}$ and $\log g$ was within the measurement errors for all but the lowest S/N objects (<10). We have excluded all objects below this S/N threshold from our final analysis to ensure we are using only the most reliable values of $T_{\rm eff}$ and $\log g$. We have found that the poorest fits to the white dwarf spectra result from low S/N (<10), not residual M star contributions from the subtraction process.

We were able to accurately fit models to 496 of the 747 binaries in our sample. Model fits could not be obtained for the remaining white dwarfs due to the low S/N of the spectrum and/or a large M dwarf flux contribution that could not be adequately removed from the spectrum. We made no attempt to determine the $T_{\rm eff}$ and $\log g$ of white dwarfs with spectral types DC, DZ, DO, or DBA. Table 4 lists the white dwarf parameters obtained from the atmospheric model fits ($T_{\rm eff}$, $\log g$, and the DA and DB subtype), as well as the cooling ages from evolutionary models of Bergeron et al. (1995).

Figure 5 plots the effective temperature distribution for the separated DA white dwarf primaries, and Figure 6 shows the $\log g$ distribution. The average $T_{\rm eff}$ of the 483 DA white dwarfs (we exclude the 13 DB dwarfs from these figures for comparison with K04) is $\sim$21,200 K. The temperature distribution of the WDMs in Figure 5 is broad, reflecting the large range of $T_{\rm eff}$ for our sample. The K04 distribution is strongly peaked at low $T_{\rm eff}$ (<10,000 K), with a high-temperature tail. Our distribution has a similar high-temperature tail but many more white dwarfs around 20,000 K. This is most likely a selection effect in the spectroscopic targeting of the WDM objects. As described above, many of our objects were targeted by the quasar pipeline, which selects many blue objects. The flux from an object selected by the quasar pipeline is dominated by the white dwarf. For an average M star companion, the white dwarf thus has to be quite hot. Systems with cooler white dwarfs are not targeted as frequently (see § 2 discussion) and/or are not recognized as spectroscopic pairs because the M dwarf masks the flux from the cool white dwarf companion.

We are conducting a parallel study in which we have already performed radial velocity follow-up on over 30 of these systems to determine their orbital periods. Preliminary results suggest that several of these systems have orbital periods that place them within the CV period gap (2 hr $< P_{\rm orb} <$ 3 hr). As each system moves into Roche lobe contact and begins mass transfer, the white dwarf is heated by the accretion process, thereby destroying any age information from the cooling of the previously detached white dwarf. Without knowing the orbital period of the hot systems, we must be cognizant of the fact that some small

TABLE 4
WHITE DWARF PARAMETERS

Name (SDSS J)	Plate	Fiber	MJD	Spectral Type (SP1 + SP2)	WD Subtype	$\sigma_{\rm WD\ Subtype}$	MS Spectral Type	log (g)	$\sigma_{\log g}$	$T_{\rm eff}$ (K)	$\sigma_{T_{\rm eff}}$ (K)	Age (yr)	Notes
001029.87+003126.2	0388	545	51793	DZ: + dM	...	...	M0	...	...	...	...	...	
001324.33−085021.4	0652	321	52138	WD: + dM	...	...	M4	...	...	...	...	...	
001726.63−002451.2	0687	153	52518	DA + dMe	3.1	0.1	M4	8.1	0.1	16507	532	1.84E+08	
001733.59+004030.4	0389	614	51795	DA + dM	2.5	0.2	M4	7.7	0.2	19888	1591	4.82E+07	
001749.24−000955.3	0389	112	51795	DA + dMe	0.7	0.0	M2	7.9	0.1	75044	0	7.10E+05	

NOTES.—Table 4 is published in its entirety in the electronic edition of the *Astronomical Journal*. A portion is shown here for guidance regarding its form and content.

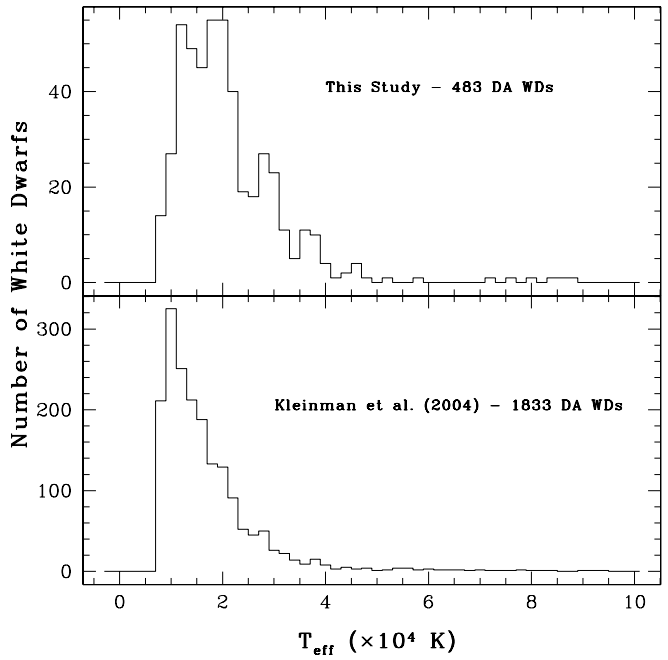

FIG. 5.—$T_{\rm eff}$ distribution of the DA white dwarfs in SDSS close binary systems (*top*) as compared to the isolated SDSS DA white dwarfs of K04 (*bottom*). The $T_{\rm eff}$ distribution of white dwarfs in close binaries is broader than in the isolated DA white dwarf sample. There are many hot white dwarfs in these systems, indicating that a large fraction of the sample is younger than the isolated DAs. See § 3 for an alternative explanation.

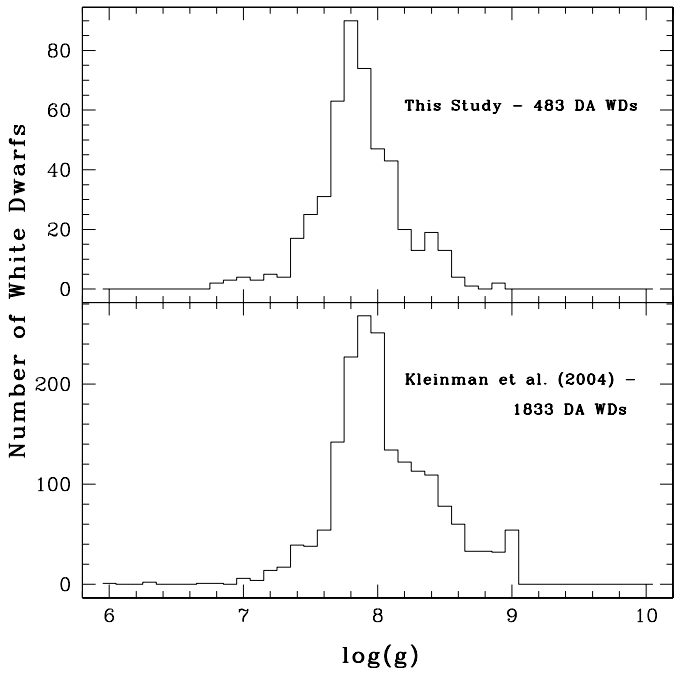

FIG. 6.—Plot of the log g distribution of the DA white dwarfs in SDSS close binary systems (*top*) as compared to the isolated SDSS white dwarfs of K04 (*bottom*). There appears to be a broader range of log g (masses) associated with close pairs than the relatively narrow distribution of log g for the field white dwarf sample, but fewer at high log g. The high log g tail is most likely an artifact of the model fits at $T_{\rm eff} < 10{,}000$ K. See K04 for details on their high log g tail.

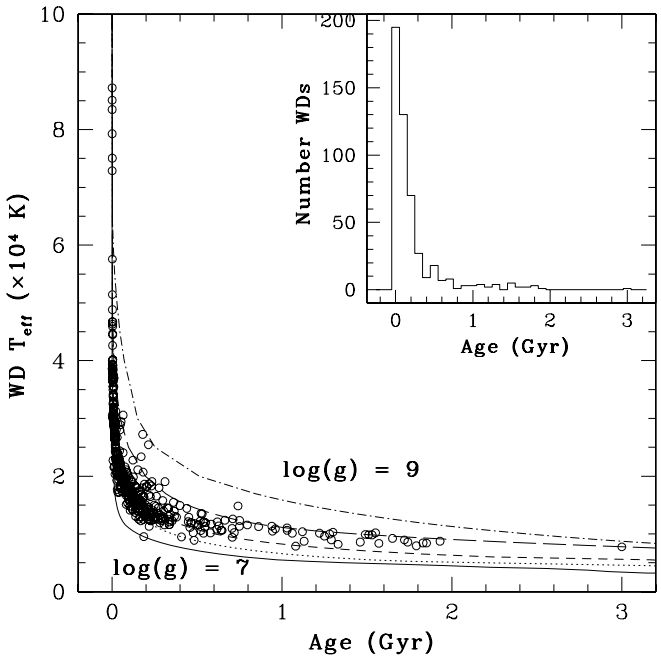

FIG. 7.—White dwarf $T_{\rm eff}$ from D. Koester's white dwarf models vs. the white dwarf age from the cooling models of P. Bergeron (see Bergeron et al. 1995). The inset panel gives the cooling age distribution of the close binaries. The majority of the measured white dwarfs are relatively young (age $< 2 \times 10^8$ yr).

number of these systems may have undergone a period of mass transfer that reheated the white dwarf. In these cases, the ages determined from the model fits can be considerably younger than the actual age of the system.

Employing the evolutionary grids (updated for SDSS colors) of Bergeron et al. (1995), we determine the age via bicubic interpolation through the evolutionary models for the $T_{\rm eff}$ and log g of each white dwarf. Figure 7 plots the $T_{\rm eff}$ versus age for the white dwarfs in our sample. Lines of constant log g are given for log $g = 7.0$, 7.5, 8.0, 8.5, and 9.0. The histogram in the upper right corner displays the resulting white dwarf age distribution.

We find that the average cooling age of DA white dwarfs with $T_{\rm eff} \sim 21{,}200$ K is approximately 0.20 Gyr. Compared to the average age implied by the numerous cool white dwarfs in the K04 sample and the age of the Galactic disk (∼7–9 Gyr; Liebert et al. 1988; Oswalt et al. 1996), these systems are quite young. They are, however, older than the 30 well-observed close binary systems described in Schreiber & Gänsicke (2003), which suggests that the SDSS is finding cooler white dwarfs in close binaries than earlier searches for these systems have revealed.

The `autofit` program returned 20 white dwarfs with low-gravity (log $g < 7$) fits, which may indicate that they are quite low mass ($M_{\rm WD} \leq 0.45\ M_{\odot}$). Most of these resulted from poor fits as a result of inadequate M dwarf flux subtraction combined with low S/N. However, five of these low-gravity objects appear to have reasonable fits but are very faint ($g \geq 20$), and as a result have very low S/N.[13] Low-mass white dwarfs in close binary systems are integral to our understanding of the mass loss and diffusion episodes in the stages leading up to the formation of white dwarfs (Benvenuto & De Vito 2004; Althaus et al. 2004). It has been suggested that a low-mass white dwarf can only be

[13] The SDSS has uncovered a variety of extreme low mass white dwarfs. See K04, Liebert et al. (2004), and Eisenstein et al. (2005) for details on these unusually low surface gravity objects.

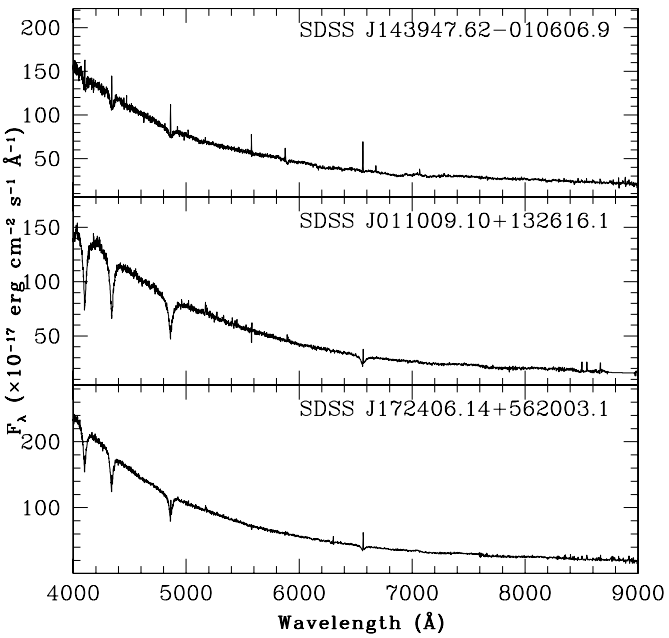

FIG. 8.—Three white dwarfs with emission in Hα, Hβ, and Hγ and no obvious optical counterpart in the red. There are 24 additional white dwarfs with similar strong emission and no optical counterpart. The feature near 5600 Å in each of the spectra is an artifact of the SDSS data reductions and is not a real feature.

formed in the presence of a binary companion (Marsh et al. 1995); a large sample of these systems would be an interesting test bed for a variety of theories. If these systems do in fact harbor low-mass white dwarfs, they would nearly double the known population of such systems. We list the fit parameters for these seven objects in Table 1 but have not included them in any of the figures pending additional spectroscopy to confirm their nature. These seven white dwarfs are identified in column (24) of Table 1.

The log g distributions of this sample and the K04 DAs are quite similar, with a fairly symmetric distribution around a peak of 7.9, as demonstrated in Figure 6. However, there are more white dwarfs with high log g in the K04 distribution (*bottom*). It is probable these high-mass white dwarfs also exist in close binary systems, but again, the lack of such systems in our sample is likely a result of our inability to distinguish them from isolated M stars. High-gravity white dwarfs have smaller radii. Paired with an average M dwarf companion, the white dwarf would contribute very little flux to the combined spectrum and would be very difficult to observe. Many such objects have probably gone undetected in SDSS spectroscopic studies and will only be revealed with UV follow-up observations.

3.1. *White Dwarfs with Emission*

Twenty-seven objects identified in this study (DA+:e) have what appear to be normal, isolated white dwarf spectral features with (in some cases, strong) hydrogen Balmer emission features in the spectra. Figure 8 shows three examples. Although there is no obvious optical signature of a close, low-mass companion other than the presence of the emission at Balmer wavelengths, the source of the emission is probably a late M dwarf (or perhaps L dwarf) companion. Most of the 27 white dwarfs are hot (>20,000 K) and bright. While M dwarfs are much larger than white dwarfs, their relatively cool temperatures result in very low luminosity at optical wavelengths, so hot white dwarfs will easily dominate the combined spectrum.

The spectra of these systems may seem to resemble low accretion rate CVs (see Szkody et al. 2004, 2005), but we can say that the emission seen in these systems is not a result of mass transfer. Emission line widths in CVs, even low $\dot{M}$ CVs, are $\sim$30–40 Å or more at their base near the continuum in Hα. In contrast, all of our systems have line widths <20 Å at the continuum. Further, many of the emission lines in CVs have structure that indicates the presence of an accretion disk, and the hydrogen emission lines are often accompanied by He I and He II lines in emission. We detect none of these signatures in the 27 objects presented here, with the exception of the two systems discussed below. Instead, the hydrogen emission features we observe are typical of emission lines produced by magnetically active M dwarf stars with strong chromospheric emission, or by M dwarfs that are subject to significant irradiation that causes excess photoionization and subsequent recombination in the hydrogen Balmer lines.

The emission we observe may be some combination of both of these processes for most of the systems in our subsample. However, two of the 27 objects (SDSS J131751.72+673159.4 and SDSS J143947.62−010606.9) show He I in emission in addition to the emission in all of the observable Balmer series lines (see Fig. 8, *top*). The simultaneous presence of H and He I lines is often produced by irradiation of an M dwarf secondary by a hot primary star, while He I is not usually observed in the emissions of normal magnetically active M dwarfs. The white dwarfs in these systems are the hottest in this subsample, making irradiation a promising candidate for producing the observed emission in these two objects.

Of particular interest is SDSS 121209.31+013627.7. The spectrum of this object, first discovered by Schmidt et al. (2003), is of a magnetic white dwarf with a 13 MG field. The emission feature at Hα is weak and not obvious in the SDSS discovery spectrum. The strong Hα emission was confirmed with follow-up spectroscopy at Apache Point Observatory[14] in 2004 March. This appears to be the first observation of a magnetic white dwarf with a nondegenerate binary companion (see Liebert et al. 2005 for details). We include this object in our tables for completeness and refer the reader to Schmidt et al. (2005) for a detailed analysis of this system.

We attempted to match all 27 white dwarfs with emission to objects observed in the Two Micron All Sky Survey (2MASS). Only eight of the 27 objects were sufficiently bright to be observed in all three 2MASS colors (JHK_S). Following the prescription outlined in Wachter et al. (2003) and Wellhouse et al. (2004), we plot the near-IR colors of the eight systems in Figure 9 and divide the plot into the same regions as Wellhouse et al. (2004) based on simulated near-IR colors. Region I is the location of single white dwarfs, while region II contains WDM binaries and region III is comprised of white dwarf–L dwarf systems. Objects in region IV may be CVs, magnetic white dwarfs, or white dwarfs with unusual atmospheric compositions.

As demonstrated in Figure 9, six of the eight objects lie within regions II and III with colors indicative of unresolved white dwarf–M dwarf or –L dwarf binary systems. The two objects in region I clearly show emission at Hα, Hβ, and Hγ, and the uncertainty in their colors suggests that these objects may belong in region III.

Hα emission has been observed in L dwarfs by groups such as Liebert et al. (2003). They argue that strong flare events with a magnetic origin are common among these low-mass objects,

[14] The Apache Point Observatory 3.5 m telescope is owned and operated by the Astrophysical Research Consortium.

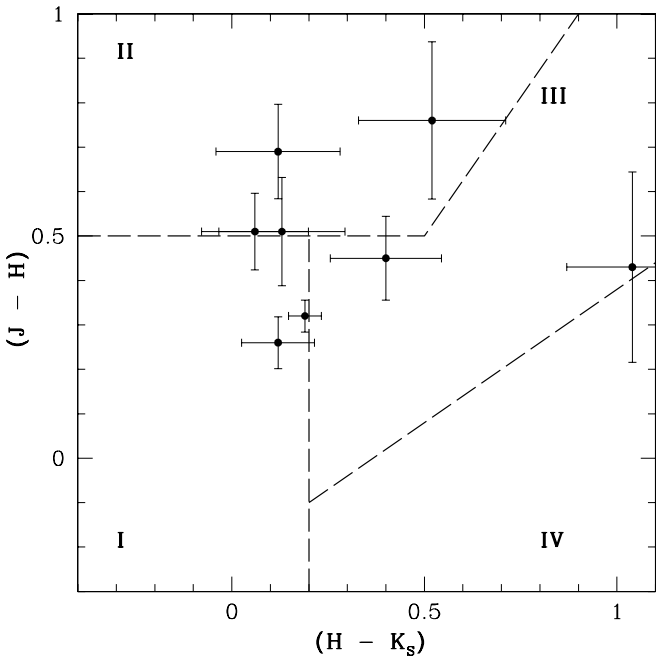

FIG. 9.—Color-color plot of eight of the 27 DA WDs with Balmer emission, recovered in 2MASS JHK_S. Objects in regions II and III have colors indicative of an unresolved low-mass companion.

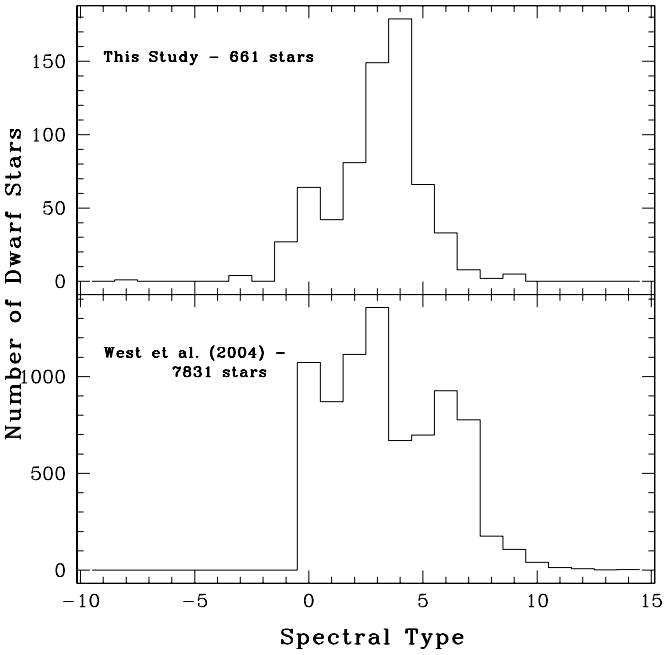

FIG. 10.—Distribution of M dwarf spectral types in WDM systems (*top*) and in W04 (*bottom*). The negative spectral type designations indicate the spectral types of the 32 K dwarf secondaries in the sample. The WDM M dwarf distribution is narrower and more symmetric than the W04 distribution. See § 4 for details.

although the mechanism for producing sustained emission is much less efficient than in earlier type M dwarfs (W04). Nevertheless, some L dwarfs do show persistent Hα emission. Thus, the low-mass companions in region III may indeed be L dwarfs.

4. THE LOW-MASS SECONDARIES

The vast majority of the secondaries in this catalog are M dwarf stars (32 are K dwarfs [dK], three are dwarf carbon stars [dC], and 15 cannot be identified [:]). The assignment of spectral type is accomplished via two typing methods: (1) a least-squares fit to template spectra of type G, K, M0–M9, and L0–L4 and (2) a weighted mean of molecular band indices as described in W04. Using these methods to predict the best-fit spectral type, each spectrum is visually inspected and the predicted spectral type updated as necessary. The uncertainty in this method is of order ± 1 spectral subtype for the M and L dwarfs. We also distinguish between early K dwarfs (K0), mid-K dwarfs (K5), and late K dwarfs (K7).

The spectral type distribution of Figure 10 is symmetric, narrow, and peaked at M4 (-1, -3, and -8 values in the figure represent K7, K5, and K0 dwarfs, respectively). This represents a convolution of the increasing mass function toward lower mass together with the decreasing visibility of lower mass stars compared to the white dwarf primaries in the optical. Thus, it probably does not give a true picture of the secondary mass function. The latest spectral type secondary we observe is M9/L0. It is likely that later L dwarf companions are hidden by the glare of the white dwarf primary and may have been overlooked as binaries, although the active ones could be identified by their hydrogen Balmer emission as described in § 3.1 (without, however, revealing their spectral type). White dwarfs with inactive, very low mass secondaries may well be present in the large SDSS white dwarf catalogs of K04 and Eisenstein et al. (2005), just as high-mass and/or very cool white dwarf primaries may be present in the large SDSS M dwarf catalog of W04 (see Fig. 10, *bottom*). Infrared photometry and spectroscopy would help to identify white dwarf binaries with very late type companions as discussed in § 3.1.

The selection effects associated with the low-mass secondaries become apparent when compared with the M dwarf distribution of W04. The W04 study includes 7831 spectroscopically identified M dwarf stars. As displayed in Figure 10, the W04 distribution is quite broad compared to the WDM distribution. The W04 sample includes many more early and late M dwarfs, whereas these objects were likely selected against in the WDM sample. The W04 study concentrated only on M dwarfs, which accounts for the sharp cutoff at zero (M0) in their distribution. As with our sample, given the uncertainty in spectral type it is possible that some of the M0 dwarfs in their study are late K dwarfs.

4.1. *M Dwarf Activity*

Collisionally induced emission at hydrogen Balmer wavelengths (Hα, Hβ, etc.) is formed in the magnetically heated chromosphere of the star. The Hα equivalent width is used to characterize magnetic activity in M dwarfs (Hawley et al. 1996). We use the trapezoidal integration technique outlined in W04 to sum the flux in Hα under the emission feature. We label a star as active if it has an Hα equivalent width greater than 1.0 Å.[15] The W04 sample was put through more rigorous selection criteria than the WDM sample because the isolated M star spectra, uncontaminated by the presence of binary companions, were generally of higher quality than our separated M star spectra, and the sheer number of M stars in the SDSS required a method other than the visual inspection of thousands of M star spectra. With the smaller number of M stars in the WDM sample, each spectrum

[15] There is more detail involved in the determination of activity in M stars than is presented here. We refer the reader to W04 for a more rigorous discussion of our M dwarf activity classification method.

TABLE 5
M Dwarf Parameters

Name (SDSS J) (1)	Plate (2)	Fiber (3)	MJD (4)	Spectral Type (SP1 + SP2) (5)	WD Subtype (6)	MS Spectral Type (7)	Hα EW (Å) (8)	$\sigma_{H\alpha\ EW}$ (Å) (9)	TiO5 (10)	σ_{TiO5} (11)	CaH1 (12)	σ_{CaH1} (13)	CaH2 (14)	σ_{CaH2} (15)
001029.87+003126.2	0388	545	51793	DZ:+dM	...	M0	−1.76	0.41	0.72	0.00	0.85	0.08	0.70	0.04
001324.33−085021.4	0652	321	52138	WD:+dM	...	M4	2.46	0.72	0.50	0.08	0.58	0.12	0.58	0.07
001726.63−002451.2	0687	153	52518	DA+dMe	3.1	M4	1.47	0.31	0.45	0.04	1.04	0.07	0.45	0.03
001733.59+004030.4	0389	614	51795	DA+dM	2.5	M4	−0.28	0.26	0.44	0.03	0.89	0.06	0.44	0.02
001749.24−000955.3	0389	112	51795	DA+dMe	0.7	M2	3.02	0.12	0.70	0.02	0.85	0.02	0.61	0.01

Name (SDSS J) (1)	CaH3 (16)	σ_{CaH3} (17)	TiO8 (18)	σ_{TiO8} (19)	Hα Continuum (Å) (20)	$\sigma_{H\alpha}$ Continuum (Å) (21)	$r-i$ (22)	log (χ) (23)	$L_{H\alpha}/L_{bol}$ (24)	log ($L_{H\alpha}/L_{bol}$) (25)	Notes (MS)[a] (26)	Notes (other) (27)
001029.87+003126.2	1.24	0.05	0.95	0.08	2.74	0.05	0.67	−3.83				
001324.33−085021.4	0.66	0.07	0.76	0.07	1.54	0.04	1.51	−4.24	1.42E−04	−3.85		
001726.63−002451.2	0.79	0.04	0.91	0.03	4.49	0.06	1.51	−4.24	8.46E−05	−4.07		
001733.59+004030.4	0.73	0.03	0.89	0.02	3.62	0.04	1.51	−4.24	...	...		
001749.24−000955.3	0.79	0.02	0.99	0.01	16.60	0.08	1.03	−4.00	3.02E−04	−3.52		

Notes.—Table 5 is published in its entirety in the electronic edition of the *Astronomical Journal*. A portion is shown here for guidance regarding its form and content.

[a] Double asterisks indicate that the spectral type is lower limit. The white dwarf could not be subtracted, resulting in earlier (bluer) spectral type identification.

can be examined visually to confirm the presence of emission. Only those M star secondaries in which the equivalent width of the Hα emission feature was measured to be greater than 1.0 Å and the emission could be confirmed visually were included in the analysis of active stars.

The equivalent width of Hα depends on the local continuum flux in the region near Hα. The equivalent width changes through the M dwarf sequence due to the rapidly changing continuum flux and is not representative of the true strength of activity of an individual M dwarf. Hence, we measure the strength of activity as a ratio of the luminosity at Hα ($L_{H\alpha}$) to the bolometric luminosity (L_{bol}) of the star. This value does not depend on the shape of the local continuum; rather, it is a representation of the radiative strength of the magnetically driven activity with respect to the total radiative output of the star. We use the distance-independent method from Walkowicz et al. (2004) and West et al. (2005) to calculate $L_{H\alpha}/L_{bol}$. This eliminates the uncertainties that would be introduced by using distances calculated from either the white dwarf or the M dwarf.

In Table 5 we provide the rough (visual) identification of the pair, the measured white dwarf subtype, the measured main-sequence star spectral type and subtype ($\sigma \sim \pm 1$ spectral subtype), the Hα equivalent width and the associated uncertainty (cols. [5]–[9]). A variety of molecular band head measurements and their uncertainties are given in columns (10)–(19), along with a measure of the Hα continuum and Hα luminosity of the M dwarf (cols. [20]–[21]). The $r-i$ color and log (χ) factor (West et al. 2005), activity strength ($L_{H\alpha}/L_{bol}$), and log of the activity strength [log ($L_{H\alpha}/L_{bol}$)] for the active M dwarfs are given in columns (22)–(25).

Figure 11 compares the mean activity strength of the WDM and W04 samples. The activity strength observed in the early M dwarfs in the WDM sample is the same as the activity strength in the W04 early M dwarfs. The magnetic activity in early M dwarfs still depends on rotation as in the FGK stars, since a solar-type dynamo can still be present when the star has a radiative core and convective envelope. In close binary systems, the secondary is either rotating synchronously with the system or is in the process of being spun up. In either case, the M dwarf is probably spinning more rapidly than an average field M dwarf, resulting in an increased fraction of active M stars (see the next paragraph's discussion), but the mechanism that creates the emission is the same. Therefore, we expect that the strength of the activity should also be similar. At later spectral types (∼M4 and later), M dwarfs become fully convective, and a rotationally

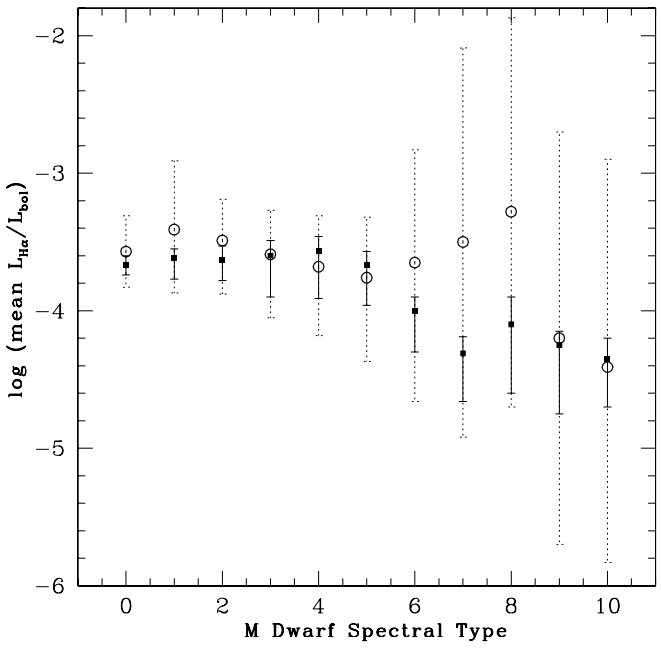

Fig. 11.—Log of the mean activity strength [log(mean $L_{H\alpha}/L_{bol}$)] vs. M dwarf spectral type for the WDM sample of active M dwarfs with Hα EW > 1.0 Å (*open circles, dotted error bars*). The same relation is plotted for the W04 sample of SDSS M dwarfs (*filled squares, solid error bars*). The WDM sample shows the same activity strength in the early spectral type M dwarfs as the W04 sample. The activity strength of the WDMs decreases toward later spectral types with respect to the W04 M dwarfs in the well-populated spectral type bins. There is evidence for an increase in activity strength at late spectral types.

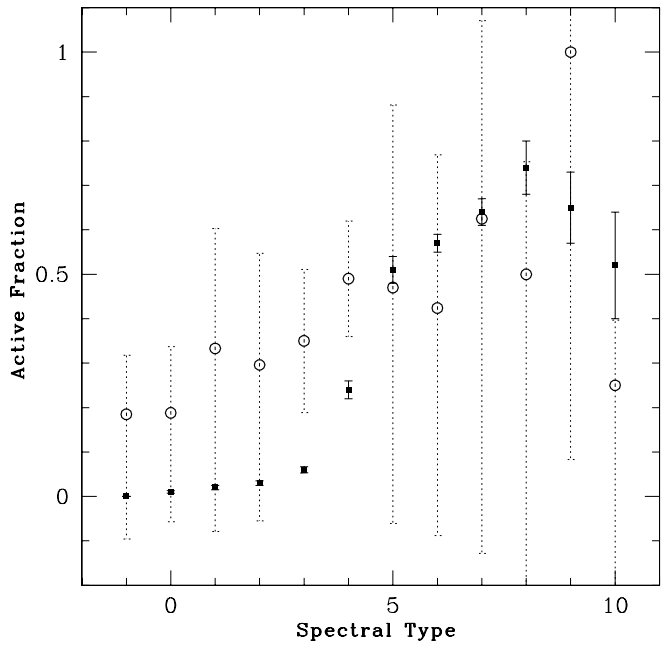

FIG. 12.—Fraction of active M dwarfs in the WDM systems (*open circles, dotted error bars*) as compared to the active fraction of M dwarf stars in the W04 study (*filled squares, solid error bars*). Although the fraction of active M dwarf stars per spectral type bin is larger for the M dwarfs in WDM systems, the trend toward a larger fraction of active M dwarfs at later spectral types is confirmed. The larger fraction of active M dwarfs at early spectral types is most likely due to the M dwarf being spun up by the close white dwarf companion. The disparity between the two samples at late spectral types is due to the small number of late spectral type M dwarfs in the WDM sample. The W04 study only used M dwarfs, which accounts for the lack of K dwarf spectral types in their sample.

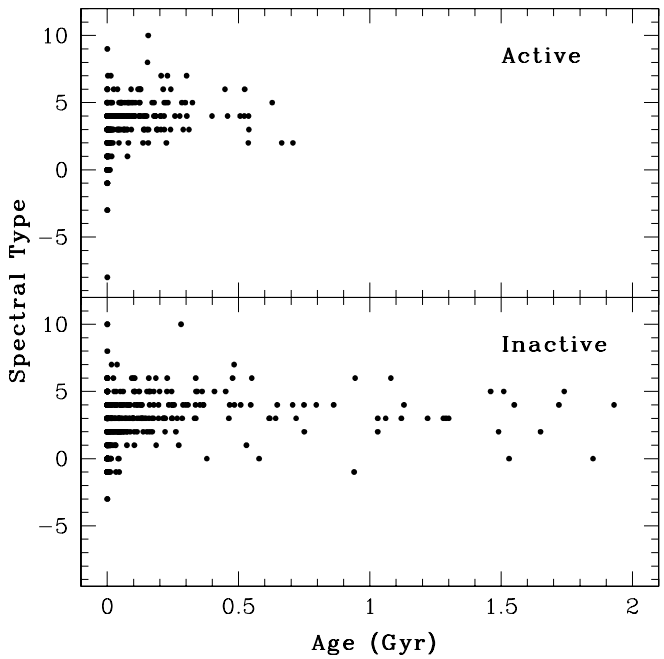

FIG. 13.—*Top*: M/K dwarf spectral type vs. white dwarf age for the active (Hα EW $>$ 1.0 Å) M dwarfs. *Bottom*: Same relation for the inactive (Hα EW $<$ 1.0 Å) M dwarfs. There is an obvious paucity of old, active M dwarfs, confirming the trend toward decreasing activity with increasing age. See § 4 for details.

driven dynamo should play a lesser role in the observed activity. In these stars the observed activity is also comparable to the activity strength of the W04 M dwarfs; this suggests that the driver behind the activity in mid-type M dwarfs in both types of system is probably the same. There is evidence of an increase in activity strength in the late-type M dwarfs in binaries with respect to the activity strength observed in field M dwarfs, but it is clear that we require more late-type M dwarfs in our WDM sample to further investigate this trend.

As expected from isolated M dwarf studies, the fraction of active stars increases with decreasing temperature (Hawley et al. 1996; W04). Figure 12 illustrates that the fraction of active stars among the WDM binaries (*open circles, dotted error bars*) is significantly larger at every spectral type compared to the extensive W04 SDSS results (*filled squares, solid error bars*). The larger fraction of active M dwarf secondaries at early types (M0–M3) may be connected to membership in a close binary system. As discussed above, the magnetic activity in early M dwarfs still depends on rotation, as in the FGK stars; therefore, the secondary is either rotating synchronously with the system or is in the process of being spun up. The M dwarf in a close binary is probably spinning more rapidly than an average field M dwarf, resulting in a larger fraction of active M dwarfs at early spectral types. As with the single-star sample, the M dwarfs in the WDM sample exhibit a sharp increase in the active fraction near this spectral type. The monotonic increase in active fraction with decreasing mass has previously been attributed to an age effect such that the activity lasts longer at later types, although the physical reason for this is not yet clear (Hawley et al. 1996; W04). We can examine this potential age effect using the ages of the white dwarfs in the WDM systems.

W04 and A. A. West et al. (2006, in preparation) demonstrate that the fraction of active M7 dwarfs decreases with vertical distance from the midplane of the Galaxy. This implies an age effect. Those stars in orbits farther from the midplane are older, due to the timescales involved in scattering them from the midplane of the disk where they were born to their current locations. We do not have a large enough sample to perform a similar comparison using the vertical distances of the WDM systems; since we have the cooling ages, we can directly compare the magnetic activity of our M dwarfs to their ages.

Figure 13 plots the M dwarf spectral type versus the companion white dwarf's age. The top panel plots only those M/K dwarfs deemed active (Hα EW $>$ 1.0 Å). The bottom panel plots the rest of the (inactive) M/K dwarfs in our sample. The striking difference between these two plots is the obvious lack of old (>0.8 Gyr) M dwarfs in the top panel. On average, in the well-populated spectral type bins, there are more older inactive M dwarfs than active M dwarfs. This appears to confirm the findings of W04 and A. A. West et al. (2006, in preparation).

This has interesting implications for close binaries. First consider the early M dwarfs. The observed activity in these stars is tied to a rotationally driven dynamo that is enhanced by the synchronous rotation of the binary. It therefore follows that we should see active early M dwarfs of all ages if the activity solely depends on rotation. Figure 13 shows that there are no old active early M dwarfs in these systems. This suggests that there is some mechanism that switches off the activity at a given age or over some period of time regardless of whether a rotationally driven dynamo is present. This phenomenon appears to be responsible for the lack of activity in the mid-late M dwarfs, where a different (turbulent) dynamo is at work. It appears that regardless of the dynamo mechanism, the activity in M dwarfs is a function of age.

Further, if activity is a function of age, it is curious that we observe many young, inactive M dwarfs. Silvestri et al. (2005)

obtained a similar result with M dwarfs in common proper motion WDM binary systems. Compared to the results of Hawley et al. (1996; see their Figs. 6 and 7), Silvestri et al. (2005) found many inactive M stars in wide binaries at colors, masses, and ages for which activity was found to be ubiquitous in cluster M dwarfs. W04 show that nearly all young M7s (those closest to the midplane of the Galaxy, $z < 50$ pc) are active, and yet there are many young, late M dwarfs in our sample that are clearly inactive. Is there some mechanism in WDM binaries that prevents activity at particular ages from being pervasive? This appears to be a property that is unique to M dwarfs in binary systems. Although more late-type M dwarfs in binaries are required to investigate this further, it is clear that although they are similar in some respects to field M dwarfs, M dwarfs in binary systems with white dwarf companions have some curious differences that are not well understood.

5. CONCLUSIONS

We have compiled a data set of nearly 750 close binary systems, the largest sample to date of systems with a white dwarf primary. The typical low-mass secondaries to the white dwarfs are M dwarfs, with an average spectral type of M4. There is a small number of white dwarfs with K dwarf and dwarf carbon star secondaries in our sample.

The average temperature of the white dwarfs in the study is $\sim$21,100 K, but the distribution is broad with a high-temperature tail, similar to the DA white dwarf distribution of K04. The peak $T_{\rm eff}$ of the WDM white dwarf distribution suggests that the majority of these pairs are younger than those in the isolated white dwarf sample of K04, although this may be due in part to several selection effects associated with the WDM sample. It is also possible that some of the hot systems have undergone a period of mass transfer as they evolve through the CV period gap. These systems would appear much younger due to the reheating of the white dwarf and subsequent destruction of age information from the white dwarf cooling times.

We find the M dwarfs in WDM binaries have similar activity strengths to those observed in large samples of isolated M dwarf stars (Hawley et al. 1996; W04), but a significantly larger fraction of the WDM binary M dwarfs appear to be active. This is most likely a result of tidal interaction and synchronous rotation induced by the presence of the close binary companion. The oldest M dwarfs in our sample are inactive (Hα EW < 1.0 Å), confirming the trend in M dwarf stars toward less activity with increasing age, as described in Hawley et al. (1996).

Follow-up spectroscopy and photometry is in progress to determine the orbital periods and parameters of a small subset of this sample ($\sim$30) and is reported in N. M. Silvestri et al. (2006a, in preparation) along with the radial velocities and kinematics of the entire sample. Our investigation of the magnetic white dwarf properties of this sample (Lemagie et al. 2005) is presented in N. M. Silvestri et al. (2006b, in preparation). We are continuing to search for these close systems in the latest plates and anticipate the addition of several hundred more WDM systems to this sample before the conclusion of the survey, bringing the known sample of close white dwarf+dM binary systems to more than 1000.

This work was supported by NSF AST 02-05875 (N. M. S., S. L. H., P. S.) and Los Alamos National Laboratory LDRD program 20030486DR (J. A. S, P. M. M.). Funding for the creation and distribution of the SDSS Archive has been provided by the Alfred P. Sloan Foundation, the Participating Institutions, the National Aeronautics and Space Administration, the National Science Foundation, the US Department of Energy, the Japanese Monbukagakusho, and the Max Planck Society. The SDSS Website is available at http://www.sdss.org.

The SDSS is managed by the Astrophysical Research Consortium for the Participating Institutions. The Participating Institutions are the University of Chicago, Fermilab, the Institute for Advanced Study, the Japan Participation Group, The Johns Hopkins University, the Korean Scientist Group, Los Alamos National Laboratory, the Max Planck Institute for Astronomy, the Max Planck Institute for Astrophysics, New Mexico State University, the University of Pittsburgh, the University of Portsmouth, Princeton University, the United States Naval Observatory, and the University of Washington.

REFERENCES

Abazajian, K., et al. 2003, AJ, 126, 2081
———. 2004, AJ, 128, 502
———. 2005, AJ, 129, 1755
Adelman-McCarthy, J. K., et al. 2006, ApJS, 162, 38 (DR4)
Althaus, L. G., et al. 2004, MNRAS, 347, 125
Benvenuto, O. G., & De Vito, M. A. 2004, MNRAS, 352, 249
Bergeron, P., Saumon, D., & Wesemael, F. 1995, ApJ, 443, 764
Dobbie, P. D., Burleigh, M. R., Levan, A. J., Barstow, M. A., Napiwotzki, R., Holberg, J. B., Hubeny, I., & Howell, S. B. 2005, MNRAS, 357, 1049
Eisenstein, D., et al. 2005, ApJ, submitted
Fan, X. 1999, AJ, 117, 2528
Finley, D. S., Koester, D., & Basri, G. 1997, ApJ, 488, 375
Fukugita, M., Ichikawa, T., Gunn, J. E., Doi, M., Shimasaku, K., & Schneider, D. P. 1996, AJ, 111, 1748
Gunn, J. E., et al. 1998, AJ, 116, 3040
———. 2005, AJ, submitted
Hawley, S. L., Gizis, J. E., & Reid, I. N. 1996, AJ, 112, 2799
Hawley, S. L., et al. 2002, AJ, 123, 3409
Hillwig, T. C., Honeycutt, R. K., & Robertson, J. W. 2000, AJ, 120, 1113
Hogg, D. W., Schlegel, D. J., Finkbinder, D. P., & Gunn, J. E. 2001, AJ, 122, 2129
Ivezić, Z., et al. 2004, Astron. Nachr., 325, 583
Kleinman, S. J., et al. 2004, ApJ, 607, 426 (K04)
Lemagie, M. P., Silvestri, N. M., Hawley, S. L., Schmidt, G., Liebert, J., & Wolfe, M. A. 2005, BAAS, 205, 103.05
Liebert, J., Bergeron, P., Eisenstein, D., Harris, H. C., Kleinman, S. J., Nitta, A., & Krzesinski, J. 2004, ApJ, 606, L147
Liebert, J., Dahn, C., & Monet, D. 1988, ApJ, 332, 891
Liebert, J., et al. 2003, AJ, 125, 343
———. 2005, AJ, 129, 2376
Lupton, R. H., et al. 1999, AJ, 118, 1406
———. 2001, in ASP Conf. Ser. 238, Astronomical Data Analysis Software and Systems X, ed. F. R. Harnden, Jr., F. A. Primini, & H. E. Payne (San Francisco: ASP), 269
Luyten, W. J. 1963, Proper Motion Survey with the Forty-Eight Inch Telescope (Minneapolis: Univ. Minnesota Press)
Marsh, T. R. 2000, NewA Rev., 44, 119
Marsh, T. R., Dhillon, V. S., & Duck, S. R. 1995, MNRAS, 275, 828
Maxted, P. F. L., et al. 2004, MNRAS, 355, 1143
Morales-Rueda, L., et al. 2005, MNRAS, 359, 648
Oswalt, T. D., Smith, J. A., Wood, M. A., & Hintzen, P. 1996, Nature, 382, 692
Pier, J. R., et al. 2003, AJ, 125, 1559
Raymond, S. N., et al. 2003, AJ, 125, 2621
Schlegel, D. J., Finkbinder, D. P., & Davis, M. 1998, ApJ, 500, 525
Schmidt, G. D., Szkody, P., Silvestri, N. M., Cushing, M. C., Liebert, J., & Smith, P. 2005, ApJ, 630, L173
Schmidt, G. D., et al. 2003, ApJ, 595, 1101
Schreiber, M. R., & Gänsicke, B. T. 2003, A&A, 406, 305
Schultz, G., Zuckerman, B., & Becklin, E. E. 1996, ApJ, 460, 402
Sion, E. M., Greenstein, J. L., Landstreet, J. D., Liebert, J., Shipman, H. L., & Wegner, G. A. 1983, ApJ, 269, 253
Silvestri, N. M., Oswalt, T. D., & Hawley, S. L. 2002, AJ, 124, 1118
Silvestri, N. M., Oswalt, T. D., Wood, M. A., Smith, J. A., Reid, I. N., & Sion, E. M. 2001, AJ, 121, 503

Silvestri, N. M., et al. 2005, AJ, 129, 2428
Smith, J. A., Silvestri, N. M., Oswalt, T. D., Harris, H. C., Kleinman, S. J., Munn, J. A., Nitta, A., & Rudkin, M. A. 2004, in ASP Conf. Ser. 334, 14th European Workshop on White Dwarfs (San Francisco: ASP), 127
Smith, J. A., et al. 2002, AJ, 123, 2121
Smolčić, V., et al. 2004, ApJ, 615, L141
Stoughton, C., et al. 2002, AJ, 123, 485 (EDR)
Szkody, P., et al. 2003, AJ, 126, 1499
———. 2004, AJ, 128, 1882
———. 2005, AJ, 129, 2386
Tucker, D., et al. 2005, AJ, submitted
Vennes, S., Thorstensen, J. R., & Polomski, E. F. 1999, ApJ, 523, 386
Wachter, S., Hoard, D. W., Hansen, K. H., Wilcox, R. E., Taylor, H. M., & Finkelstein, S. L. 2003, ApJ, 586, 1356
Walkowicz, L. M., Hawley, S. L., & West, A. A. 2004, PASP, 116, 1105
Wellhouse, J. W., Hoard, D. W., Howell, S. B., & Wachter, S. 2004, BAAS, 205, 103.04
West, A. A., Walkowicz, L. M., & Hawley, S. L. 2005, PASP, 117, 706
West, A. A., et al. 2004, AJ, 128, 426 (W04)
York, D. G., et al. 2000, AJ, 120, 1579